PERGAMON

International Journal of Heat and Mass Transfer 42 (1999) 2967–2980

International Journal of HEAT and MASS TRANSFER

Transient coupled radiative and conductive heat transfer in an absorbing, emitting and scattering medium

Heping Tan[a,*], Liming Ruan[a], Xinlin Xia[a], Qizheng Yu[a], Timothy W. Tong[b]

[a] *School of Energy Science and Engineering, Harbin Institute of Technology, Harbin, 150001, China*
[b] *Department of Mechanical Engineering, Colorado State University, Fort Collins, CO 80523-1374, U.S.A.*

Received 20 April 1998; in final form 25 September 1998

Abstract

On the basis of our previous papers, the redistribution of radiative energy in the case of isotropic scattering is investigated and the radiative transfer coefficient (RTC) under specular reflection in an absorbing, emitting and isotropic scattering parallel slab is derived. Considering both multi-reflection and multi-scattering in the derivation, the RTC can accommodate various boundary conditions under specular reflection. By accumulating the RTC for specular reflection boundary and that for diffuse reflection boundary linearly, the RTC are calculated. The validity and high precision of the formula for the RTC are confirmed by comparing with references. The effects of single-scattering albedo ω, Planck number Np and refractive index of STM n_m on the transient coupled heat transfer in a one-dimensional isotropic scattering medium are reviewed for: (a) two semi-transparent boundaries; and (b) one semi-transparent boundary and one opaque boundary. The presented calculation and formula for the redistribution of the scattering energy can also be applied to other radiative calculations, such as total radiative exchange area or total radiative transfer coefficient in multi-dimensional isotropic scattering media.

Nomenclature

$A_{k,T_i} = \int_{\Delta\lambda_k} I_{b,\lambda}(T_i)\,d\lambda / \int_0^\infty I_{b,\lambda}(T_i)\,d\lambda$, fractional spectral emissive power of spectral band k at nodal temperature T_i
C unit heat capacity [J m^{-3} K^{-1}]
h_1, h_2 heat transfer coefficient at surfaces of S_1 and S_2, respectively [W m^{-2} K^{-1}]
L slab thickness [m]
$n_{m,k}$, $n_{rf,k}$ refractive index of STM and reference, respectively, relative to the spectral band $k(\Delta\lambda_k)$
Np Planck number, $Np = \lambda_c/(4Ln_m^2\sigma T_{rf2}^3)$
NB total number of spectral bands
NM total number of the nodes (control volumes)
q^{cd}, q^{cv}, q^{r} heat fluxes of thermal conduction, convection heat transfer and radiative transfer, respectively [W m^{-2}]
$S_{-\infty}$, $S_{+\infty}$ black surfaces representing the surroundings
$(S_iS_j)_k$, $(S_iV_j)_k$, $(V_iV_j)_k$ radiative heat transfer coefficient in non-scattering media relative to the spectral band $k(\Delta\lambda_k)$
$\lfloor S_iS_j \rfloor_k$, $\lfloor S_iV_j \rfloor_k$, $\lfloor V_iV_j \rfloor_k$ radiative heat transfer coefficient in isotropic scattering media relative to the spectral band $k(\Delta\lambda_k)$
t physical time [s]
$t^*(L) = Fo(L) = \lambda_c t/(CL^2)$, dimensionless time
t_s^* steady-state dimensionless time
T_i temperature of the node i [K]
T_{rf} reference temperature [K]
T_0 initial temperature [K]
V_i volume relative to node i.

Greek symbols
α absorption coefficient [m^{-1}]
γ transmissivity of surfaces
Δt, Δt^* time interval and dimensionless time interval, respectively
ε emissivity of surfaces
η $\eta = 1-\omega$
θ angle of reflection
θ_c critical angle of reflection
Θ dimensionless normalized temperature $(T-T_{rf1})/(T_{rf2}-T_{rf1})$
κ extinction coefficient [m^{-1}]

* Corresponding author.

0017–9310/99/$ - see front matter
PII: S0017-9310(98)00347-0

λ wavelength [μm]
λ_c phonic thermal conductivity [W m^{-1} K^{-1}]
μ $\mu = \cos\theta$, direction cosine
ρ_i^d, ρ_i^s diffuse and specular reflectivity components, respectively, $i = 1$ or 2
σ Stefan–Boltzmann constant
σ_s scattering coefficient [m^{-1}]
τ, τ_0 optical depth and optical thickness, respectively
Φ_i^r radiative source term of the node i
ω single-scattering albedo.

Subscripts
a absorbed fraction in the overall radiative heat transfer coefficient
k relative to spectral band k.
s scattered quota in the overall radiative heat transfer coefficient
1, 2 refer to frontiers S_1 and S_2, respectively
$-\infty$, $+\infty$ refer to frontiers $S_{-\infty}$ and $S_{+\infty}$, respectively.

Superscripts
cd, cv, r, t refer to thermal conduction, convection, radiation and total, respectively
d, s diffuse and specular reflection, respectively
d+s combined diffuse and specular reflection
m, $m+1$ time step.

1. Introduction

The combined radiation–conduction heat transfer is apparent in various engineering applications for semi-transparent materials (STM), such as the glass industry, molten salt media, fibrous materials, infrared heating as well as the utilization of solar energy, etc. Early studies of this subject were reviewed in detail by Viskanta and Anderson [1] and by Kunc et al. [2]. It has attracted further research in recent years, as to the combined heat transfer with multi-dimension [3–7], under transient state [3–6, 8–14], or with refractive index greater than unity [11, 15, 16], in a scattering medium [6, 7, 12, 14–16, 17–28], as well as with various boundary conditions and various radiative characteristics of the boundary [15–18, 20–24, 26].

On solving one-dimensional radiative transfer in a scattering medium, Machali [21] and Machali and Madkour [22] investigated the radiative transfer in a plane-parallel slab of an absorbing, emitting and scattering medium for combined diffuse and specular reflection boundaries. Siegel [17, 18], Kudo [20] and Ganapol [23] investigated the radiative transfer in a plane-parallel slab of an absorbing, emitting and isotropic scattering medium for transparent or semi-transparent boundaries. Lin and Tsai [24] and Siewert [26] investigated the coupled radiation–conduction heat transfer in an absorbing, emitting and scattering medium for combined diffuse and specular reflection boundaries. Spuckler and Siegel [15, 16] studied the heat transfer in a composite layer medium, which is composed of two layers of different isotropic scattering STM, the refractive indexes of which are both greater than unity. Recently studies of this subject have been reviewed in detail by Siegel [29].

By employing the ray tracing method, the overall radiative transfer coefficients (RTC) between two surface elements, between a surface element and a control volume or between two control volumes, in a one-dimensional STM, were presented for three different boundary conditions under specular reflection: (a) two opaque boundaries [10]; (b) two semi-transparent boundaries [11]; and (c) a semi-transparent boundary S_1 and an opaque one S_2 [30]. In these researches, however, the scattering effect was neglected.

In this paper, the scattering effect, various kinds of radiative characteristics of the boundaries, the spectral effect and the effect of refractive index are considered comprehensively.

2. Physical model and governing equation

The energy equation for transient coupled heat transfer of radiation–conduction in a homogeneous absorbing, emitting and isotropic scattering medium slab is given by

$$\rho C_P\, \partial T/\partial \tau = -\mathrm{div}(\mathbf{q}^{cd} + \mathbf{q}^{r}) \quad (1)$$

where $\mathbf{q}^{cd}$, $\mathbf{q}^{r}$ are conductive and radiative flux densities. One boundary surface S_1 of the slab is semi-transparent, the other one S_2 is opaque. The slab thickness is L and the slab is between two black surfaces ($S_{-\infty}$ and $S_{+\infty}$) which indicate environments, whose temperatures are $T_{S_{-\infty}}$ and $T_{S_{+\infty}}$, respectively. The slab is divided into NM control volumes (nodes) along its thickness, i indicates one node (see Fig. 1). The time interval is from t $(=m\Delta t)$ to $t+\Delta t$ $(=[m+1]\Delta t)$, so the implicit discrete equation is obtained as

$$C\Delta x(T_i^{m+1} - T_i^m)/\Delta t = [\lambda_{c,ie}^{m+1}(T_{i+1}^{m+1} - T_i^{m+1}) + \lambda_{c,iw}^{m+1}(T_{i-1}^{m+1} - T_i^{m+1})]/\Delta x + \Phi_i^{r,m+1} \quad (2)$$

where $\lambda_{c,ie}$, $\lambda_{c,iw}$ are harmonic mean media thermal conductivity at the interface 'ie' (between control volumes i and $i+1$) and 'iw' (between control volumes $i-1$ and i).

The extinction coefficient κ, absorption coefficient α, the scattering coefficient σ_s, the refractive index n_m and the surface reflectivity ρ are approximately simplified as that in a series of rectangular spectral bands. The total number of spectral bands is NB. BOP indicates the 'opaque' zone and BST indicates the 'semi-transparent' zone.

When $k \in BST$, the boundary conditions at the semi-transparent boundary S_1 and the opaque boundary S_2 are as follows, respectively,

$$\text{Boundary surface } S_1 \quad q^{cd} = q^{cv} \quad (3a)$$

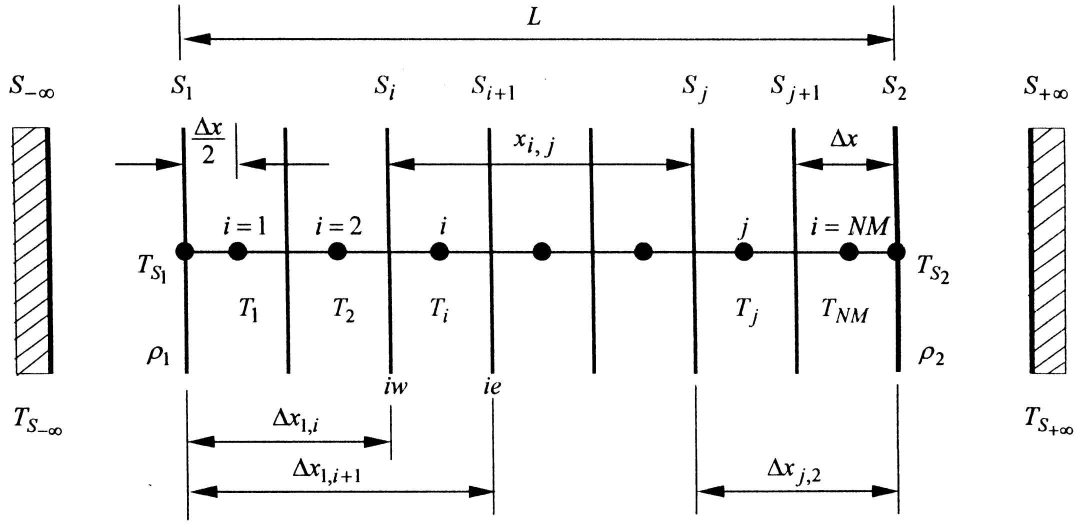

Fig. 1. The infinite slab of STM modeling by the control volume method.

Table 1
Optical characteristics of the different glasses used

	Spectrum A					Spectrum B			
k	λ (μm)	$n_{m,k}$	$\rho_{1,k}$	$\rho_{2,k}$	κ_k (m^{-1})	λ (μm)	$n_{m,k}$	$\rho_{1,k}=\rho_{2,k}$	κ_k (m^{-1})
1	0.5–2.7	1.5	0.04	0.97	10	0.5–1.0	1.5 or 3.0	0.04	10
2	2.7–4.5	1.5	0.04	0.97	1000	1.0–2.7	1.5 or 3.0	0.04	100
3	4.5–50	1.5	0.06	0.97	5000	2.7–4.3	1.5 or 3.0	0.04	1000
4						4.3–10.3	1.5 or 3.0	0.06	10 000
5						10.3–50.0	1.5 or 3.0	0.15	10 000

Boundary surface S_2 $\quad q^{\mathrm{r}}_{S_2}+q^{\mathrm{cd}} = q^{\mathrm{r}}_{S_2\to S_{+\infty}}+q^{\mathrm{cv}}$ (3b)

where q^{cd} is the heat conduction flux density between the boundary node and the adjacent node. q^{cv} is the heat convection flux density between the boundary node and the environment. $q^{\mathrm{r}}_{S_2}$ is the radiative flux density between the boundary surface node S_2 and all internal nodes, including the surrounding black surface $S_{-\infty}$ (because in the semi-transparent zone, radiative ray can pass through the boundary S_1, transferring heat to $S_{-\infty}$ directly). $q^{\mathrm{r}}_{S_2\to S_{+\infty}}$ is the radiative flux density between S_2 and the black surface $S_{+\infty}$ indicating the environment. The discrete equation of equation (3b) is shown as follows

$$\sigma\sum_{k\in BST} n^2_{m,k}\left\{\varepsilon_{2,k}[S_2S_{-\infty}]^{\mathrm{s}}_{k,\mathrm{t-o}}(A_{k,T_{S_{-\infty}}}T^4_{S_{-\infty}}-A_{k,T_{S_2}}T^4_{S_2})\right.$$
$$\left.+\sum_{j=1}^{NM}\varepsilon_{2,k}[S_2V_j]^{\mathrm{s}}_{k,\mathrm{t-o}}(A_{k,T_j}T^4_j-A_{k,T_{S_2}}T^4_{S_2})\right\}+2\lambda_{\mathrm{c},NM}$$
$$\times(T_{NM}-T_{S_2})/\Delta x = \sigma\sum_{k=1}^{NB} n^2_{\mathrm{rf},k}\varepsilon_{2,k}$$
$$\times(A_{k,T_{S_2}}T^4_{S_2}-A_{k,T_{S_{+\infty}}}T^4_{S_{+\infty}})+h_2(T_{S_2}-T_{S_{+\infty}}) \quad (4)$$

where $A_{k,T_i}=\int_{\Delta\lambda_k}I_{\mathrm{b},\lambda}(T_i)\,\mathrm{d}\lambda/\int_0^\infty I_{\mathrm{b},\lambda}(T_i)\,\mathrm{d}\lambda$ is the fractional spectral emissive power of the spectral band k at the nodal temperature T_i. If the coefficient of heat transfer h_i ($i=1,2$) in equation (4) approaches infinity, the surface temperature of the medium is equal to the surrounding temperature $T_{S_1}=T_{S_{-\infty}}$, $T_{S_2}=T_{S_{+\infty}}$, equation (4) is changed to the first kind of boundary condition.

When S_1 is the semi-transparent boundary and S_2 is the opaque boundary, Φ^{r}_i can be expressed as

$$\Phi^{\mathrm{r}}_i=\sigma\sum_{k\in BST} n^2_{m,k}\left\{\varepsilon_{2,k}[S_2V_i]^{\mathrm{s}}_{k,\mathrm{t-o}}(A_{k,T_{S_2}}T^4_{S_2}-A_{k,T_i}T^4_i)\right.$$
$$+\sum_{j=1}^{NM}[V_jV_i]^{\mathrm{s}}_{k,\mathrm{t-o}}(A_{k,T_j}T^4_j-A_{k,T_i}T^4_i) \quad 1\leqslant i\leqslant NM$$

$$+[V_iS_{-\infty}]^{\mathrm{s}}_{k,\mathrm{t\text{-}o}}(A_{k,T_{S_{-\infty}}}T^4_{S_{-\infty}}-A_{k,T_i}T_i^4)\Big\}. \tag{5}$$

If both boundaries are opaque or semi-transparent, the radiative source term is given in refs. [10, 11].

3. Radiative transfer coefficient

In equations (4) and (5), $[S_iS_j]^{\mathrm{s}}_k$, $[S_iV_j]^{\mathrm{s}}_k$ and $[V_iV_j]^{\mathrm{s}}_k$ are RTC of surface to surface, surface to control volume and control volume to control volume, respectively, in an absorbing, emitting, isotropic scattering medium. In the following, the RTC in an absorbing–emitting medium is discussed first, then the RTC in an absorbing, emitting, isotropic scattering medium under specular reflection is deduced.

3.1. Absorbing–emitting media

Under specular reflection, because the incident angle is equal to the reflecting angle, two rays with different launching angles cannot intersect each other (Fig. 2). The extinction function of a ray with an arbitrary launching angle can be yielded by tracing this ray, then the spectral coefficients $(S_1S_j)^{\mathrm{s}}_k$, $(S_2S_j)^{\mathrm{s}}_k$ and $(S_iS_j)^{\mathrm{s}}_k$ can be calculated by integrating between $0\sim\pi/2$. From the energy conservation equations

$$(S_1V_i)^{\mathrm{s}}_{k,\mathrm{t\text{-}o}}=(S_1S_i)^{\mathrm{s}}_{k,\mathrm{t\text{-}o}}-(S_1S_{i+1})^{\mathrm{s}}_{k,\mathrm{t\text{-}o}} \tag{6}$$

$$\begin{aligned}(V_iV_j)^{\mathrm{s}}_{k,\mathrm{t\text{-}o}}&=(S_{i+1}S_j)^{\mathrm{s}}_{k,\mathrm{t\text{-}o}}\\&\quad-(S_iS_j)^{\mathrm{s}}_{k,\mathrm{t\text{-}o}}-(S_{i+1}S_{j+1})^{\mathrm{s}}_{k,\mathrm{t\text{-}o}}+(S_iS_{j+1})^{\mathrm{s}}_{k,\mathrm{t\text{-}o}}.\end{aligned} \tag{7}$$

So we have

$$\begin{aligned}(V_iV_j)^{\mathrm{s}}_{k,\mathrm{t\text{-}o}}&=2\{[F_k(\kappa_kx_{i+1,j})-F_k(\kappa_kx_{i+1,j+1})\\&\quad-F_k(\kappa_kx_{i,j})+F_k(\kappa_kx_{i,j+1})]_0^{\mu_c}\\&\quad+\rho^{\mathrm{s}}_{2,k}[F_k(\kappa_kx_{i+1,2}+\kappa_kx_{2,j+1})-F_k(\kappa_kx_{i+1,2}+\kappa_kx_{2,j})\\&\quad-F_k(\kappa_kx_{i,2}+\kappa_kx_{2,j+1})+F_k(\kappa_kx_{i,2}+\kappa_kx_{2,j})]_0^{\mu_c}\\&\quad+[F_k(\kappa_kx_{i,1}+\kappa_kx_{1,j})-F_k(\kappa_kx_{i,1}+\kappa_kx_{1,j+1})\\&\quad-F_k(\kappa_kx_{i+1,1}+\kappa_kx_{1,j})+F_k(\kappa_kx_{i+1,1}+\kappa_kx_{1,j+1})]_0^{\mu_c}\\&\quad+\rho^{\mathrm{s}}_{2,k}[F_k(\kappa_kx_{i,1}+\tau_{0k}+\kappa_kx_{2,j+1})-F_k(\kappa_kx_{i,1}\\&\quad+\tau_{0k}+\kappa_kx_{2,j})-F_k(\kappa_kx_{i+1,1}+\tau_{0k}\\&\quad+\kappa_kx_{2,j+1})+F_k(\kappa_kx_{i+1,1}+\tau_{0k}+\kappa_kx_{2,j})]_0^{\mu_c}\\&\quad+[F_k(\kappa_kx_{i+1,j})-F_k(\kappa_kx_{i+1,j+1})-F_k(\kappa_kx_{i,j})\\&\quad+F_k(\kappa_kx_{i,j+1})]^1_{\mu_c}+\rho^{\mathrm{s}}_{2,k}[F_k(\kappa_kx_{i+1,2}\\&\quad+\kappa_kx_{2,j+1})-F_k(\kappa_kx_{i+1,2}+\kappa_kx_{2,j})\\&\quad-F_k(\kappa_kx_{i,2}+\kappa_kx_{2,j+1})+F_k(\kappa_kx_{i,2}+\kappa_kx_{2,j})]^1_{\mu_c}\\&\quad+\rho^{\mathrm{s}}_{1,k}[F_k(\kappa_kx_{i,1}+\kappa_kx_{1,j})-F_k(\kappa_kx_{i,1}+\kappa_kx_{1,j+1})\\&\quad-F_k(\kappa_kx_{i+1,1}+\kappa_kx_{1,j})+F_k(\kappa_kx_{i+1,1}+\kappa_kx_{1,j+1})]^1_{\mu_c}\\&\quad+\rho^{\mathrm{s}}_{1,k}\rho^{\mathrm{s}}_{2,k}[F_k(\kappa_kx_{i,1}+\tau_{0k}+\kappa_kx_{2,j+1})-F_k(\kappa_kx_{i,1}\\&\quad+\tau_{0k}+\kappa_kx_{2,j})-F_k(\kappa_kx_{i+1,1}+\tau_{0k}\\&\quad+\kappa_kx_{2,j+1})+F_k(\kappa_kx_{i+1,1}+\tau_{0k}+\kappa_kx_{2,j})]^1_{\mu_c}\}\end{aligned} \tag{8}$$

$$(S_{-\infty}S_2)^{\mathrm{s}}_{k,\mathrm{t\text{-}o}}=2(n_{m,k}/n_{\mathrm{rf},k})^2\gamma_{1,k}\varepsilon_{2,k}[F_k(\tau_{0k})]^1_{\mu_c} \tag{9}$$

$$\begin{aligned}(S_{-\infty}V_i)^{\mathrm{s}}_{k,\mathrm{t\text{-}o}}&=2(n_{m,k}/n_{\mathrm{rf},k})^2\gamma_{1,k}[F_k(\kappa_kx_{1,i})-F_k(\kappa_kx_{1,i+1})\\&\quad+\rho^{\mathrm{s}}_{2,k}F_k(\tau_{0k}+\kappa_kx_{2,i+1})-\rho^{\mathrm{s}}_{2,k}F_k(\tau_{0k}+\kappa_kx_{2,i})]^1_{\mu_c}\end{aligned} \tag{10}$$

$$\begin{aligned}(S_2V_i)^{\mathrm{s}}_{k,\mathrm{t\text{-}o}}&=2\{[F_k(\kappa_kx_{2,i+1})\\&\quad-F_k(\kappa_kx_{2,i})+F_k(\tau_{0k}+\kappa_kx_{1,i})\\&\quad-F_k(\tau_{0k}+\kappa_kx_{1,i+1})]_0^{\mu_c}+[F_k(\kappa_kx_{2,i+1})\\&\quad-F_k(\kappa_kx_{2,i})+\rho^{\mathrm{s}}_{1,k}F_k(\tau_{0k}+\kappa_kx_{1,i})\\&\quad-\rho^{\mathrm{s}}_{1,k}F_k(\tau_{0k}+\kappa_kx_{1,i+1})]^1_{\mu_c}\}.\end{aligned} \tag{11}$$

In the above equations

$$[F_k(z)]_0^{\mu_c}=\int_0^{\mu_c}\mu\exp(-z/\mu)/[1-\rho^{\mathrm{s}}_{2,k}\exp(-2\tau_{0k}/\mu)]\,\mathrm{d}\mu \tag{12a}$$

$$[F_k(z)]^1_{\mu_c}=\int_{\mu_c}^1\mu\exp(-z/\mu)/[1-\rho^{\mathrm{s}}_{1,k}\rho^{\mathrm{s}}_{2,k}\exp(-2\tau_{0k}/\mu)]\,\mathrm{d}\mu \tag{12b}$$

$$\tau_{0k}=\kappa_kd\quad\mu_c=\cos\theta_c\quad\theta_c=\sin^{-1}(n_{\mathrm{rf},k}/n_{m,k}) \tag{12c}$$

where the superscript 's' indicates specular reflection, and the subscript 't–o' indicates that one side is the semi-

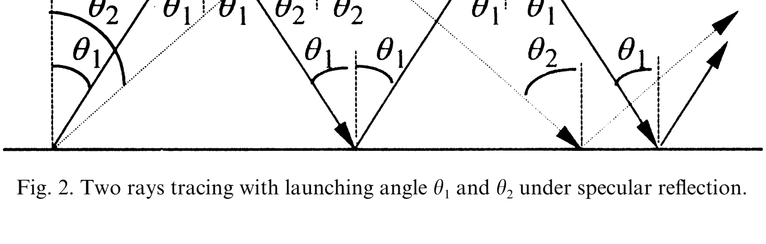

Fig. 2. Two rays tracing with launching angle θ_1 and θ_2 under specular reflection.

transparent boundary and the other side is the opaque boundary, and

$$\begin{aligned} n^2_{\mathrm{rf},k}(S_{-\infty}S_2)^{\mathrm{s}}_{k,\mathrm{t\text{–}o}} &= n^2_{m,k}\varepsilon_{2,k}(S_2S_{-\infty})^{\mathrm{s}}_{k,\mathrm{t\text{–}o}} \\ \varepsilon_{2,k}(S_2V_i)^{\mathrm{s}}_{k,\mathrm{t\text{–}o}} &= (V_iS_2)^{\mathrm{s}}_{k,\mathrm{t\text{–}o}} \\ n^2_{\mathrm{rf},k}(S_{-\infty}V_i)^{\mathrm{s}}_{k,\mathrm{t\text{–}o}} &= n^2_{m,k}(V_iS_2)^{\mathrm{s}}_{k,\mathrm{t\text{–}o}} \\ (V_iV_j)^{\mathrm{s}}_{k,\mathrm{t\text{–}o}} &= (V_jV_i)^{\mathrm{s}}_{k,\mathrm{t\text{–}o}}. \end{aligned} \tag{13}$$

Subscript 'o–o' indicates that both sides are opaque boundaries, the spectral RTC are given in ref. [10]. Subscript 't–t' indicates that both sides are semi-transparent boundaries, the spectral RTC are given by [11]

$$\begin{aligned} &(S_iS_j)^{\mathrm{s}}_{k,\mathrm{o\text{–}o}},\quad (S_iV_j)^{\mathrm{s}}_{k,\mathrm{o\text{–}o}},\quad (V_iV_j)^{\mathrm{s}}_{k,\mathrm{o\text{–}o}} \\ &\quad (S_i = S_1, S_2 \quad S_j = S_1, S_2) \\ &(S_iS_j)^{\mathrm{s}}_{k,\mathrm{t\text{–}t}},\quad (S_iV_j)^{\mathrm{s}}_{k,\mathrm{t\text{–}t}},\quad (V_iV_j)^{\mathrm{s}}_{k,\mathrm{t\text{–}t}} \\ &\quad (S_i = S_{-\infty}, S_{+\infty} \quad S_j = S_{-\infty}, S_{+\infty}). \end{aligned}$$

3.2. Absorbing–emitting–isotropic scattering media

In equations (8)–(11), $(S_iS_j)^{\mathrm{s}}_k$, $(S_iV_j)^{\mathrm{s}}_k$ and $(V_iV_j)^{\mathrm{s}}_k$ are given without considering the effect of scattering, $\kappa_k = \alpha_k$. For the scattering media, $\kappa_k = \alpha_k + \sigma_{\mathrm{s},k}$, the radiative energy represented by $(S_iS_j)^{\mathrm{s}}_k$, $(S_iV_j)^{\mathrm{s}}_k$ and $(V_iV_j)^{\mathrm{s}}_k$ will redistribute. Suppose $\eta = 1-\omega$, ω is the single-scattering albedo. In the following deduction, subscripts 'o–o', 't–o', 't–t', 'k' and superscript 's' will be omitted, because the deduction and formula of RTC are independent on the properties of boundaries and spectrum. Subscripts 'a' and 's' indicate the absorbing and scattering, respectively.

3.2.1. First-order scattering

Notice there is only reflection at the boundary of the scattering medium, which has been considered in the above deduction. Considering the first-order scattering, the corresponding quota of absorption will be (S_iS_j), (V_iS_j), $\eta\cdot(S_iV_j)$ and $\eta\cdot(V_iV_j)$, respectively; the remaining part will be scattered.

$$\begin{aligned} &[V_iV_j]^{\mathrm{1st}}_{\mathrm{a}} = (V_iV_j)\eta \quad [V_iS_j]^{\mathrm{1st}}_{\mathrm{a}} = (V_iS_j) \\ &[S_iV_j]^{\mathrm{1st}}_{\mathrm{a}} = (S_iV_j)\eta \quad [S_iS_j]^{\mathrm{1st}}_{\mathrm{a}} = (S_iS_j) \\ &[V_iV_j]^{\mathrm{1st}}_{\mathrm{s}} = (V_iV_j)\omega \quad [S_iV_j]^{\mathrm{1st}}_{\mathrm{s}} = (S_iV_j)\omega \\ &(S_i, S_j = S_1, S_2 \quad \text{or } S_i, S_j = S_{-\infty}, S_2 \\ &\quad \text{or } S_i, S_j = S_{-\infty}, S_{+\infty}) \end{aligned} \tag{14}$$

where the superscript '1st' indicates the first-order scattering.

3.2.2. Second-order scattering

The RTC between two control volumes (i to j) can be calculated as

$$[V_iV_j]^{\mathrm{2nd}}_{\mathrm{a}} = [V_iV_j]^{\mathrm{1st}}_{\mathrm{a}} + \sum_{l_2=1}^{NM} \omega(V_iV_{l_2})\cdot\eta(V_{l_2}V_j)$$

where the superscript '2nd' indicates the second-order scattering. On the right-hand-side of this expression, the first item indicates the absorbed energy quota by element j, which emits from element i and considering only the first-order scattering. The second item indicates the absorbed energy quota by element j after the first-order scattering of the element l_2 ($l_2 = 1, 2, \ldots, NM$), so after second-order scattering, the RTC is given by

$$\begin{aligned} &[V_iS_j]^{\mathrm{2nd}}_{\mathrm{a}} = [V_iS_j]^{\mathrm{1st}}_{\mathrm{a}} + \sum_{l_2=1}^{NM}(V_iV_{l_2})(V_{l_2}S_j)\omega \\ &[S_iV_j]^{\mathrm{2nd}}_{\mathrm{a}} = [S_iV_j]^{\mathrm{1st}}_{\mathrm{a}} + \sum_{l_2=1}^{NM}(S_iV_{l_2})(V_{l_2}V_j)\omega\eta \\ &[S_iS_j]^{\mathrm{2nd}}_{\mathrm{a}} = [S_iS_j]^{\mathrm{1st}}_{\mathrm{a}} + \sum_{l_2=1}^{NM}(S_iV_{l_2})(V_{l_2}S_j)\omega \\ &[V_iV_j]^{\mathrm{2nd}}_{\mathrm{s}} = \sum_{l_2=1}^{NM}(V_iV_{l_2})(V_{l_2}V_j)\omega^2 \\ &[S_iV_j]^{\mathrm{2nd}}_{\mathrm{s}} = \sum_{l_2=1}^{NM}(S_iV_{l_2})(V_{l_2}V_j)\omega^2 \\ &\quad (S_i, S_j = S_1, S_2 \quad \text{or } S_i, S_j = S_{-\infty}, S_2 \\ &\quad \text{or } S_i, S_j = S_{-\infty}, S_{+\infty}). \end{aligned} \tag{15}$$

3.2.3. (n+1)th-order scattering

$$\begin{aligned} [V_iV_j]^{(n+1)\mathrm{th}}_{\mathrm{a}} &= [V_iV_j]^{n\mathrm{th}}_{\mathrm{a}} + \omega^n\eta\cdot\sum_{l_2=1}^{NM}(V_iV_{l_2}) \\ &\cdot\left\{\sum_{l_3=1}^{NM}(V_{l_2}V_{l_3})\cdot\left\{\sum_{l_4=1}^{NM}(V_{l_3}V_{l_4})\right.\right. \\ &\cdot\left\{\sum_{l_5=1}^{NM}(V_{l_4}V_{l_5})\cdot\left[\sum_{l_6=1}^{NM}(V_{l_5}V_{l_6})\cdots\right.\right. \\ &\left.\left.\left.\left.\cdot\left[\sum_{l_{n+1}=1}^{NM}(V_{l_n}V_{l_{n+1}})(V_{l_{n+1}}V_j)\right]\right]\right\}\right\}\right\} \end{aligned} \tag{16a}$$

$$\begin{aligned} [V_iS_j]^{(n+1)\mathrm{th}}_{\mathrm{a}} &= [V_iS_j]^{n\mathrm{th}}_{\mathrm{a}} + \omega^n\cdot\sum_{l_2=1}^{NM}(V_iV_{l_2}) \\ &\cdot\left\{\sum_{l_3=1}^{NM}(V_{l_2}V_{l_3})\cdot\left\{\sum_{l_4=1}^{NM}(V_{l_3}V_{l_4})\right.\right. \\ &\cdot\left\{\sum_{l_5=1}^{NM}(V_{l_4}V_{l_5})\cdot\left[\sum_{l_6=1}^{NM}(V_{l_5}V_{l_6})\cdots\right.\right. \\ &\left.\left.\left.\left.\cdot\left[\sum_{l_{n+1}=1}^{NM}(V_{l_n}V_{l_{n+1}})(V_{l_{n+1}}S_j)\right]\right]\right\}\right\}\right\} \end{aligned} \tag{16b}$$

$$\begin{aligned} [S_iV_j]^{(n+1)\mathrm{th}}_{\mathrm{a}} &= [S_iV_j]^{n\mathrm{th}}_{\mathrm{a}} + \omega^n\eta\cdot\sum_{l_2=1}^{NM}(S_iV_{l_2})\cdot\left\{\sum_{l_3=1}^{NM}(V_{l_2}V_{l_3})\right. \\ &\cdot\left\{\sum_{l_4=1}^{NM}(V_{l_3}V_{l_4})\cdot\left\{\sum_{l_5=1}^{NM}(V_{l_4}V_{l_5})\cdot\left[\sum_{l_6=1}^{NM}(V_{l_5}V_{l_6})\cdots\right.\right.\right. \end{aligned}$$

$$\cdot\left[\sum_{l_{n+1}=1}^{NM}(V_{l_n}V_{l_{n+1}})(V_{l_{n+1}}V_j)\right]\Bigg]\Bigg\}\Bigg\}\Bigg\}\Bigg\} \quad (16c)$$

$$[S_iS_j]_a^{(n+1)\text{th}} = [S_iS_j]_a^{n\text{th}} + \omega^n\cdot\sum_{l_2=1}^{NM}(S_iV_{l_2})$$
$$\cdot\left\{\sum_{l_3=1}^{NM}(V_{l_2}V_{l_3})\cdot\left\{\sum_{l_4=1}^{NM}(V_{l_3}V_{l_4})\right.\right.$$
$$\cdot\left\{\sum_{l_5=1}^{NM}(V_{l_4}V_{l_5})\cdot\left[\sum_{l_6=1}^{NM}(V_{l_5}V_{l_6})\cdots\right.\right.$$
$$\cdot\left[\sum_{l_{n+1}=1}^{NM}(V_{l_n}V_{l_{n+1}})(V_{l_{n+1}}S_j)\right]\Bigg]\Bigg\}\Bigg\}\Bigg\}\Bigg\} \quad (16d)$$

$$[V_iV_j]_s^{(n+1)\text{th}} = \omega^{n+1}\cdot\sum_{l_2=1}^{NM}(V_iV_{l_2})$$
$$\cdot\left\{\sum_{l_3=1}^{NM}(V_{l_2}V_{l_3})\cdot\left\{\sum_{l_4=1}^{NM}(V_{l_3}V_{l_4})\right.\right.$$
$$\cdot\left\{\sum_{l_5=1}^{NM}(V_{l_4}V_{l_5})\cdot\left[\sum_{l_6=1}^{NM}(V_{l_5}V_{l_6})\cdots\right.\right.$$
$$\cdot\left[\sum_{l_{n+1}=1}^{NM}(V_{l_n}V_{l_{n+1}})(V_{l_{n+1}}V_j)\right]\Bigg]\Bigg\}\Bigg\}\Bigg\}\Bigg\} \quad (16e)$$

$$[S_iV_j]_s^{(n+1)\text{th}} = \omega^{n+1}\cdot\sum_{l_2=1}^{NM}(S_iV_{l_2})$$
$$\cdot\left\{\sum_{l_3=1}^{NM}(V_{l_2}V_{l_3})\cdot\left\{\sum_{l_4=1}^{NM}(V_{l_3}V_{l_4})\right.\right.$$
$$\cdot\left\{\sum_{l_5=1}^{NM}(V_{l_4}V_{l_5})\cdot\left[\sum_{l_6=1}^{NM}(V_{l_5}V_{l_6})\cdots\right.\right.$$
$$\cdot\left[\sum_{l_{n+1}=1}^{NM}(V_{l_n}V_{l_{n+1}})(V_{l_{n+1}}V_j)\right]\Bigg]\Bigg\}\Bigg\}\Bigg\}\Bigg\}. \quad (16f)$$

3.2.4. *Energy equilibrium during deduction*

In the previous deduction, a basic condition has been implied that the energy absorbed and scattered must be of unit quantity. Such as $\lfloor V_iV_j \rfloor$, after the first-order scattering, the scattering part is $[V_iV_j]_s^{1\text{st}} = (V_iV_j)\omega$. After the second-order scattering, the redistribution of scattering energy is as follows

$$(V_iV_j)\omega\{[(V_jS_1)+(V_jS_2)] + [(V_jV_1)+(V_jV_2)+\cdots+(V_jV_{NM})]\cdot(\omega+\eta)\}$$

the quota absorbed by boundaries S_1, S_2 and all control volumes is expressed as

$$(V_iV_j)\omega\{[(V_jS_1)+(V_jS_2)] + [(V_jV_1)+(V_jV_2)+\cdots+(V_jV_{NM})]\cdot\eta\}.$$

The RTC in the absorbing–emitting medium has the following expression

$$\sum_{j\,\text{inclu}\,i}\varepsilon_{i,k}(S_iS_j)_k + \sum_j \varepsilon_{i,k}(S_iV_j)_k = \varepsilon_{i,k}S_i$$

$$\sum_{j\,\text{inclu}\,i}(V_iV_j)_k + \sum_j (V_iS_j)_k = 4\kappa_kV_i. \quad (17)$$

So when calculating the RTC in the isotropic scattering medium, the RTC in the absorbing–emitting medium must be normalized first

$$(V_iV_j)_k^* = (V_iV_j)_k/(4\kappa_kV_i) \quad (V_iS_j)_k^* = (V_iS_j)_k/(4\kappa_kV_i)$$
$$(S_iV_j)_k^* = (S_iV_j)_k/(\varepsilon_{i,k}S_i) \quad (S_iS_j)_k^* = (S_iS_j)_k/(\varepsilon_{i,k}S_i) \quad (18)$$

where the superscript '*' indicates the normalized value. The inverse operation is done after the calculation of the $(n+1)$th-order scattering and absorbing. The energy absorbed or scattered must be of unit quantity, otherwise, the total energy will increase or decrease (depending upon $4\kappa_kV_i > 1$, or < 1).

3.2.5. *Method and speed of calculation*

However, equation (16) is difficult to apply in practical calculations. As for $\lfloor V_iV_j \rfloor$, considering second-order scattering, three loops must be calculated: $i = 1 \to NM$, $j = 1 \to NM$, $l_2 = 1 \to NM$. Lately, when one more scattering is considered, one more loop will be calculated, so after the nth scattering the calculating amount is $(NM+2)^{n+1}$ (NM control volumes and two boundary surface nodes). The calculation was started with a Pentium 133, when $NM = 4$, eighth-order scattering takes 40 s, ninth-order scattering takes $40\times(NM+2) = 240$ s, tenth-order scattering takes 24 min. If the number of control volumes are very large and single-scattering albedo ω is large as well, the calculating time will be much longer. For example, when $\tau_0 = 5$, $NM = 20$, $\omega = 0.90$, after the 14th-order scattering, the sum of the normalized RTC when $i = 4$ is as follows

$$\sum_{j=1}^{NM}[V_4V_j]_a^{14\text{th},*} + [V_4S_1]_a^{14\text{th},*} + [V_4S_2]_a^{14\text{th},*} = 0.933143674$$

$$\sum_{j=1}^{NM}[V_4V_j]_s^{14\text{th},*} = 0.066856326.$$

If the sum of the normalized RTC is desired to reach 0.999999994 (the sum of the scattering quota of the first four control volumes $\leqslant \text{EPS0} = 3.0\times10^{-8}$), 104th-order scattering should be calculated. When these conditions do not change except that $\omega = 0.95$, 148th-order scattering should be calculated and when $\omega = 0.98$, 196th-order scattering should be calculated. In order to calculate more conveniently, equation (16a) is rewritten as

$$[V_iV_j]_a^{(n+1)\text{th}} = [V_iV_j]_a^{n\text{th}} + \omega^n\eta\cdot\sum_{l_{n+1}=1}^{NM}(V_iV_{l_{n+1}})$$
$$\cdot\left\{\sum_{l_n=1}^{NM}(V_{l_{n+1}}V_{l_n})\cdots\cdot\left\{\sum_{l_5=1}^{NM}(V_{l_6}V_{l_5})\right.\right.$$
$$\cdot\left\{\sum_{l_4=1}^{NM}(V_{l_5}V_{l_4})\cdot\left[\sum_{l_3=1}^{NM}(V_{l_4}V_{l_3})\right.\right.$$

$$\cdot\left[\sum_{l_2=1}^{NM}(V_{l_3}V_{l_2})(V_{l_2}V_j)\right]\Bigg]\Bigg]\Bigg\}\Bigg\}\Bigg\}. \qquad (19)$$

The calculation is started from the inside to the outside, which is programed as a subroutine and the calculation is performed in pairs (only three loops). So one more scattering will only call two more subroutines, after nth-order scattering, the amount of calculation is $2n(NM+2)^3$. For example, the calculation is started with a Pentium 166, the optical thickness is 10, $\omega = 0.8$, $\mathrm{EPS0} = 3.0\times10^{-8}$, the calculating time is shown in Table 2.

Table 2
Calculating time after nth-order scattering

Number of nodes NM	100	200	300	400
Scattering number n	73	73	73	73
Calculating time (min)	2	15	52	123

4. Radiative transfer and transient heat transfer for opaque frontiers and specified boundary temperature

4.1. *Transient coupled heat transfer for specified boundary temperature*

Frankel [27] studied the transient coupled radiative–conductive heat transfer in a one-dimensional isotropic scattering gray medium for opaque black frontiers and a specified boundary temperature. The validity of this paper is tested by this literature. Supposing the reference temperature was $T_{\mathrm{rf}} = 1000$ K, the initial temperature $T_i(t=0) = 0$, $T_{S_2} = 0$ and the dimensionless temperature $\Xi = T/T_{\mathrm{rf}}$. The conduction–radiation number was $N_{\mathrm{cr}} = \lambda_c\kappa/(4n_m^2\sigma T_{\mathrm{rf}}^3) = 0.1$, the dimensionless time $\xi = (\lambda_c/C)\kappa^2 t = 0.05$, $\omega = 0.5$, $\tau_0 = 1$ and the dimensionless spatial variable $\zeta = (\tau - \tau_0/2) - 1$. The results are shown in Tables 3 and 4. The results of ref. [27] are also shown for comparison.

The dimensionless temperatures at the dimensionless coordinates $\zeta = -0.5$, 0, 0.5, respectively, are shown in Table 3. The radiative flux densities at the dimensionless coordinates $\zeta = -1, 0, 1$, respectively, are shown in Table 4. By comparison, it is seen that the results in this paper are consistent with those of Sutton, Barker, Tsai and Frankel. Even if the girder is widely divided (control volume $NM = 50$), the time step is large ($\Delta t = 11.023705375$ s, $m = 200$), the result is also satisfactory. When $NM = 200$ and $\Delta t = 0.440948215$ s ($m = 5000$), the results in this paper are consistent with those of Frankel's [27] eighth-order approximation.

Table 3
Comparison of temperature results at three spatial locations ($\xi = 0.05$, $\Xi_i = \Xi_2 = 0$)

Investigators [12]	Dimensionless temperature		
	$\zeta = -0.5$	$\zeta = 0$	$\zeta = 0.5$
Lii and Ozisik	0.4617	0.1474	0.0277
Sutton	0.4888	0.1778	0.0591
Barker and Sutton	0.4893	0.1775	0.0588
Tsai and Lin	0.4889	0.1773	0.0588
Frankel [27]			
Fourth-order approximation	0.4996	0.1797	0.0504
Sixth-order approximation	0.4888	0.1777	0.0584
Eighth-order approximation	0.4893	0.1773	0.0587
Present study			
$m^* = 200$, $NM = 50$	0.488407	0.177040	0.058844
$m = 1000$, $NM = 100$	0.489181	0.177265	0.058717
$m = 5000$, $NM = 200$	0.489345	0.177314	0.058690

* m is the number of steps for calculating up to non-dimensional time $\xi = 0.05$, $m = 200$, $\Delta t = 11.023705375$ s, $m = 1000$, $\Delta t = 2.204741075$ s, $m = 5000$, $\Delta t = 0.440948215$ s.

Table 4
Comparison of radiative heat flux results at three spatial locations ($\xi = 0.05$, $\Xi_i = \Xi_2 = 0$)

Investigators [12]	Dimensionless radiative heat fluxes		
	$\zeta = -1$	$\zeta = 0$	$\zeta = 1$
Lii and Ozisik	1.6436	1.2529	0.9746
Sutton	1.9304	1.3305	0.8332
Barker and Sutton	1.9300	1.3314	0.8335
Tsai and Lin	1.9328	1.3292	0.8321
Frankel [27]			
Fourth-order approximation	1.9355	1.3025	0.8339
Sixth-order approximation	1.9348	1.3284	0.8317
Eighth-order approximation	1.9342	1.3289	0.8319
Present study			
$m = 200$, $NM = 50$	1.935278	1.328469	0.831680
$m = 1000$, $NM = 100$	1.934418	1.328769	0.831858
$m = 5000$, $NM = 200$	1.934218	1.328834	0.831896

4.2. *Radiative heat transfer for combined diffuse and specular reflection boundaries*

Formulas (8)–(11) are deduced for the case that both boundaries are specular reflective. When two boundaries S_1 and S_2 are diffuse and opaque, the RTC (or Radiative

Extended Exchange Area) [2] in a non-scattering medium with the consideration of multi-reflection, are calculated as follows

$$(S_1S_2)^{\mathrm{d}}_{k,\mathrm{o-o}} = \varepsilon_{2,k}(s_1s_2)_k/[1-\rho_{1,k}\rho_{2,k}(s_1s_2)^2_k] \tag{20a}$$

$$(S_1V_j)^{\mathrm{d}}_{k,\mathrm{o-o}} = [(s_1v_j)_k+\rho_{2,k}(s_1s_2)_k(v_js_2)_k]/[1-\rho_{1,k}\rho_{2,k}(s_1s_2)^2_k] \tag{20b}$$

$$(S_2V_j)^{\mathrm{d}}_{k,\mathrm{o-o}} = [(s_2v_j)_k+\rho_{1,k}(s_2s_1)_k(v_js_1)_k]/[1-\rho_{1,k}\rho_{2,k}(s_2s_1)^2_k] \tag{20c}$$

$$(V_iV_j)^{\mathrm{d}}_{k,\mathrm{o-o}} = (v_iv_j)_k + \frac{\rho_{1,k}(s_1v_i)_k\lfloor(s_1v_j)_k+\rho_{2,k}(s_1s_2)_k(s_2v_j)_k\rfloor}{1-\rho_{1,k}\rho_{2,k}(s_2s_1)^2_k} + \frac{\rho_{2,k}(s_2v_i)_k[(s_2v_j)_k+\rho_{1,k}(s_1s_2)_k(s_1v_j)_k]}{1-\rho_{1,k}\rho_{2,k}(s_2s_1)^2_k}. \tag{20d}$$

If considering the scattering effect, by substituting equation (20) into equation (16) and adopting the layout of equation (19), the RTC can be obtained.

In this paper, the RTC for combined diffuse and specular reflecting boundaries are calculated by accumulating the RTC for the specular reflecting boundary (indicated by superscript 's') and that for the diffuse reflecting boundary (indicated by superscript 'd'), linearly

$$[F_iF_j]^{\mathrm{d+s}}_{k,\mathrm{o-o}} = P_{\mathrm{refl}}\times[F_iF_j]^{\mathrm{s}}_{k,\mathrm{o-o}}+(1-P_{\mathrm{refl}})[F_iF_j]^{\mathrm{d}}_{k,\mathrm{o-o}} \quad (F_i = S_i, V_i, \quad F_j = S_j, V_j) \tag{21a}$$

where P_{refl} is the quota of the specular reflection

$$P_{\mathrm{refl}} = (\rho^{\mathrm{s}}_1+\rho^{\mathrm{s}}_2)/(\rho^{\mathrm{s}}_1+\rho^{\mathrm{d}}_1+\rho^{\mathrm{s}}_2+\rho^{\mathrm{d}}_2). \tag{21b}$$

Machali and Madkour [22] studied the radiative heat transfer for combined diffuse and specular boundaries in an absorbing, emitting and isotropic or linear anisotropic scattering gray slab. The method of this paper is verified by taking advantage of the case of an isotropic scattering medium (see Table 1 in ref. [22]) with two opaque gray boundaries, in which the heat conduction is neglected and $n_m = 1$, $\omega = 1$, boundary temperatures ($T_{S_1} = 2T_{S_2}$) are given. So take $\lambda_c = 1\times10^{-12}$ [W m^{-1} K^{-1}] and let EPS0 $= 3\times10^{-8}$, EPS1 $= 0.001$ (required precision in calculating the temperature field) in this paper. The number of control volumes NM is 300 per optical thickness for $\tau_0 = 0.01 \sim 0.1$, is 100 per optical thickness for $\tau_0 = 0.5 \sim 2$ and is 60 per optical thickness for $\tau_0 = 5$. The radiative heat flux density q^{r} at boundary S_1 is

$$q^{\mathrm{r}} = \sigma\cdot\left\{\left[\sum_{j=1}^{NM}\varepsilon_1[S_1V_j]^{\mathrm{d+s}}_{\mathrm{o-o}}T^4_{S_1}-[V_jS_1]^{\mathrm{d+s}}_{\mathrm{o-o}}T^4_j\right] + [\varepsilon_1[S_1S_2]^{\mathrm{d+s}}_{\mathrm{o-o}}T^4_{S_1}-\varepsilon_2[S_2S_1]^{\mathrm{d+s}}_{\mathrm{o-o}}T^4_{S_2}]\right\}. \tag{22}$$

The dimensionless radiative heat flux density $\tilde{q}^{\mathrm{r}}_{22}$ is as follows (subscript '22' indicates that the parameter is defined according to ref. [22])

$$\tilde{q}^{\mathrm{r}}_{22} = q^{\mathrm{r}}/[2\cdot\varepsilon_1\cdot\sigma\cdot T^4_{S_1}]. \tag{23}$$

The results, which are shown in Table 5, are consistent with those in ref. [22].

5. Radiative transfer and coupled transient heat transfer for semi-transparent frontiers

5.1. Calculated results compared with that from refs. [17, 18]

In outer space, the waste heat can only be lost from the medium with liquid (or medium with particles) by

Table 5
Comparison of the dimensionless heat fluxes for slabs

		$\tau_0 = 0.01$	$\tau_0 = 0.1$	$\tau_0 = 0.5$	$\tau_0 = 1$	$\tau_0 = 2$	$\tau_0 = 5$
(a) $\rho^{\mathrm{d}}_1 = 0$, $\rho^{\mathrm{s}}_1+\varepsilon_1 = 1.0$, $\rho^{\mathrm{d}}_2 = 0.2$, $\rho^{\mathrm{s}}_2 = 0$, $\varepsilon_2 = 0.8$							
$\varepsilon_1 = 0.2$	Ref. [22]	0.44559	0.43851	0.41229	0.38554	0.34261	0.25772
$P_{\mathrm{refl}} = 0.8$	Present study	0.445588	0.438534	0.412361	0.385597	0.342634	0.257729
$\varepsilon_1 = 0.7$	Ref. [22]	0.39661	0.37798	0.31827	0.26854	0.20591	0.12165
$P_{\mathrm{refl}} = 0.6$	Present study	0.396609	0.377999	0.318315	0.268569	0.205915	0.121657
$\varepsilon_1 = 1.0$	Ref. [22]	0.37208	0.34928	0.28067	0.22788	0.16660	0.09254
$P_{\mathrm{refl}} = 0$	Present study	0.372077	0.349277	0.280673	0.227885	0.166598	0.092541
(b) $\rho^{\mathrm{d}}_1 = 0.2$, $\rho^{\mathrm{s}}_1 = 0$, $\varepsilon_1 = 0.8$, $\rho^{\mathrm{d}}_2 = 0$, $\rho^{\mathrm{s}}_2+\varepsilon_2 = 1.0$							
$\varepsilon_2 = 0.2$	Ref. [22]	0.11140	0.10963	0.10307	0.09639	0.08565	0.06443
$P_{\mathrm{refl}} = 0.8$	Present study	0.111397	0.109634	0.103090	0.096399	0.085658	0.064432
$\varepsilon_2 = 0.7$	Ref. [22]	0.34703	0.33073	0.27848	0.23497	0.18017	0.10645
$P_{\mathrm{refl}} = 0.6$	Present study	0.347033	0.330749	0.278525	0.234998	0.180175	0.106450
$\varepsilon_2 = 1.0$	Ref. [22]	0.46509	0.43660	0.35084	0.28485	0.20824	0.11567
$P_{\mathrm{refl}} = 0$	Present study	0.465096	0.436597	0.350841	0.284856	0.208248	0.115676

means of radiation. The physical model can be simplified as, the radiative heat transfer between a one-dimensional isothermal absorbing–emitting–scattering gray medium with semi-transparent frontiers and the circumstance ($T_{S_{-\infty}} = T_{S_{+\infty}}$). Reference [17] adopted the numerical solution of an integral equation, suppose $n_m = 1$, the dimensionless radiative heat flux $\tilde{q}^{\mathrm{r}}_{17}$ is given as follows (subscript '17' indicates that the dimensionless radiative heat flux is defined according to ref. [17])

$$\tilde{q}^{\mathrm{r}}_{17} = n_m^2 \left\{ \sum_{i=1}^{NM} ([V_i S_{+\infty}]^{\mathrm{s}}_{\mathrm{t-t}} T_i^4 - [S_{+\infty} V_i]^{\mathrm{s}}_{\mathrm{t-t}} T^4_{S_{+\infty}}) \right\} \Big/ (T_i^4 - T^4_{S_{+\infty}}). \quad (24)$$

In this paper, the number of control volumes NM is from 10–20 per optical thickness, the comparison between the result of this paper and that of ref. [17] is shown in Table 6.

In the above calculation, if considering the cooling process of the medium with a liquid droplet (or medium with particles), this will be the transient combined radiation–conduction heat transfer. We solved the following problems to compare with ref. [18]:

(1) Since the conduction was neglected in ref. [18], therefore, let $\lambda_c = 1 \times 10^{-12}$ [W m^{-1} K^{-1}] in this paper.
(2) Since the reflectivities of both boundaries are zero ($\rho = 0$), the calculation may be performed by considering either diffuse or specular reflection. The medium is gray and $n_m = 1$.
(3) Convergence condition is $|\{(T_{NM/2} - T_1)/T_1\}^{m+1} - \{(T_{NM/2} - T_1)/T_1\}^m| \leqslant \mathrm{EPS2} = 0.01$.
(4) Emissivity of the medium is defined as $\bar{\varepsilon} = q^{\mathrm{r}}(\tau_0, t)/[\sigma T_m^4(t)]$ (where T_m is the integral mean temperature).

$$q^{\mathrm{r}}(\tau_0, t) = \sigma n_m^2 \left\{ \sum_{i=1}^{NM} \times ([V_i S_{+\infty}]^{\mathrm{s}}_{\mathrm{t-t}} A_{T_i} T_i^4 - [S_{+\infty} V_i]^{\mathrm{s}}_{\mathrm{t-t}} A_{T_{S_{+\infty}}} T^4_{S_{+\infty}}) \right\}. \quad (25)$$

The comparison between this paper and ref. [18] is shown in Table 7.

5.2. Transient coupled heat transfer in isotropic scattering medium for semi-transparent frontiers

The optical properties of the absorbing–emitting–scattering medium with both semi-transparent boundary surfaces are shown in Table 1 (Spectrum B). The thickness of the slab is $L = 0.5$ cm, $C = 688\,856.448$ J K^{-1} m^{-3}, $\lambda_c = 0.0043053526$ and 0.043053526 W m^{-1} K^{-1}, respectively (corresponding $Np = 0.0005$ and 0.005). Both boundary surfaces S_1 and S_2 are of convection–radiation boundary conditions. The initial temperature is $T_0 = T_{\mathrm{rf2}} = 1500$ K, $T_{S_{+\infty}} = T_{S_{-\infty}} = T_{\mathrm{rf1}} = 750$ K and the dimensionless normalized temperature is $\Theta = (T_i - T_{\mathrm{rf1}})/(T_{\mathrm{rf2}} - T_{\mathrm{rf1}})$. $NM = 100$, the dimensionless variable time step is employed in the calculation [9], $\Delta t^* = 1 - \exp(-B \cdot m)$, where $B = 0.000223$. The results of considering the influence of the scattering albedo ω, the Planck number Np and the refractive index of STM n_m on coupled radiative–conductive heat transfer, are shown in Fig. 3(a)–(d).

6. Transient coupled heat transfer for one semi-transparent boundary and one opaque frontier

6.1. Transient heat transfer in the mixed boundary condition

The optical properties of the medium, which were given in ref. [11] as 'float' glass are shown in Table 1 (Spectrum

Table 6
Dimensionless radiative heat flux $\tilde{q}^{\mathrm{r}}_{17}$ of one-dimensional isotropic scattering isothermal gray medium for semi-transparent frontiers

τ_0	Ref. [17]	Present study		Ref. [17]	Present study		Ref. [17]	Present study	
	$\omega = 0.00$			$\omega = 0.30$			$\omega = 0.60$		
0.5	0.557	$NM = 10$	0.5567913	0.449	$NM = 10$	0.4492462	0.303	$NM = 10$	0.3031370
1	0.781	$NM = 20$	0.7806161	0.667	$NM = 20$	0.6668722	0.490	$NM = 20$	0.4901975
5	0.998	$NM = 100$	0.9982444	0.924	$NM = 100$	0.9226018	0.798	$NM = 100$	0.7977136
10	1.000	$NM = 200$	0.9999929	0.933	$NM = 200$	0.9256084	0.808	$NM = 200$	0.8053395
	$\omega = 0.80$			$\omega = 0.90$			$\omega = 0.95$		
0.5	0.172	$NM = 10$	0.1724179	0.0926	$NM = 10$	0.0925892	0.0481	$NM = 10$	0.0480754
1	0.304	$NM = 20$	0.3036279	0.173	$NM = 20$	0.1725512	0.0926	$NM = 20$	0.0926239
5	0.637	$NM = 100$	0.6355296	0.470	$NM = 100$	0.4703325	0.317	$NM = 100$	0.3164436
10	0.659	$NM = 200$	0.6576291	0.518	$NM = 200$	0.5182605	0.389	$NM = 200$	0.3894618

Table 7
Emissivity of one-dimensional isotropic scattering gray media for semi-transparent frontiers $\bar{\varepsilon}$ (EPS0 = 3.0E−08, EPS1 = 0.001, EPS2 = 0.01)

τ_0	Ref. [18]	Present study		Ref. [18]	Present study		Ref. [18]	Present study	
	$\omega = 0.30$			$\omega = 0.60$			$\omega = 0.80$		
1	0.662	$NM = 20$	0.6622064	0.489	$NM = 20$	0.4887345	0.304	$NM = 20$	0.3033532
3	0.830	$NM = 60$	0.8295321	0.722	$NM = 60$	0.7222619	0.555	$NM = 60$	0.5548919
5	0.753	$NM = 100$	0.7517080	0.696	$NM = 100$	0.6954319	0.592	$NM = 100$	0.5920237
10	0.544	$NM = 100$	0.5444467	0.529	$NM = 100$	0.5289561	0.496	$NM = 100$	0.4958588
14	0.437	$NM = 140$	0.4372308	0.430	$NM = 140$	0.4301855	0.414	$NM = 140$	0.4141381
		$NM = 300$	0.4365481		$NM = 300$	0.4295252		$NM = 300$	0.4135254
	$\omega = 0.90$			$\omega = 0.95$			$\omega = 0.98$		
1	0.173	$NM = 20$	0.1725083	0.093	$NM = 20$	0.0926179	0.039	$NM = 20$	0.0387639
3	0.379	$NM = 60$	0.3792496	0.232	$NM = 60$	0.2322984	0.107	$NM = 60$	0.1074556
5	0.456	$NM = 100$	0.4563982	0.313	$NM = 100$	0.3131194	0.161	$NM = 100$	0.1613661
10	0.440	$NM = 200$	0.4401863	0.360	$NM = 200$	0.3602210	0.233	$NM = 200$	0.2333974
14	0.385	$NM = 140$	0.3852582	0.338	$NM = 140$	0.3381247	0.248	$NM = 140$	0.2475437
		$NM = 300$	0.3847264		$NM = 300$	0.3377129		$NM = 300$	0.2473206

A), the thickness of the slab is $L = 10$ cm, $\lambda_c = 0.8610705$ W m^{-1} K^{-1} (corresponding to $Np = 0.005$), $C = 861\,070.5$ J K^{-1} m^{-3}. The initial temperature is $T_0 = 1500$ K, $T_{S_{+\infty}} = T_{\rm rf2} = 1500$ K, $T_{S_{-\infty}} = T_{\rm rf1} = 750$ K. S_2 is an opaque frontier and its temperature is given by supposing that $Bi_2(x = L) = \infty$, so $T_{S_2} = T_{S_{+\infty}}$. S_1 is a semi-transparent frontier with convection and radiation boundary conditions, supposing that $Bi_1(x = 0) = 0.1$. $NM = 100$, $\Delta t^* = 1-\exp(-B\cdot m)$. The calculated results of coupled heat transfer of radiation–conduction are shown in Fig. 4(a)–(c). The results for two opaque boundaries are shown in these figures as well for comparison, where the curve 'o–o' indicates two opaque boundaries, 't–o' indicates one opaque boundary and one semi-transparent boundary.

6.2. Transient transfer with imposed exchange boundary conditions

The optical properties of the medium are shown in Table 1 (Spectrum B), $n_{k,m} = 1.5$. The thickness of the slab is $L = 0.5$ cm, the initial temperature is $T_0 = T_{\rm rf2} = 1500$ K, $T_{S_{-\infty}} = T_{S_{+\infty}} = T_{\rm rf1} = 750$ K, $Np(t^* = 0) = 0.005$ (corresponding to $\lambda_c = 0.04305353$ W m^{-1} K^{-1}). Both boundary surfaces are of convection–radiation boundary conditions and $Bi_1(L/2) = Bi_2(L/2) = 0.05$. Considering three different boundaries: (a) opaque/opaque frontiers 'o–o'; (b) semi-transparent/opaque frontiers 't–o'; and (c) semi-transparent/semi-transparent frontiers 't–t', the calculating temperature profiles ($\omega = 0$ and $\omega = 0.9$) in the scattering medium slab are shown in Fig. 5(a)–(c), respectively. The calculating parameters are as follows: $C = 688\,856.48$ J K^{-1} m^{-3}, $NM = 100$, the dimensionless time step $\Delta t^*(L/2) = 0.0001$ and dimensionless time $t^*(L/2) = Fo(L/2)$ are 0.01, 0.05, 0.1, 0.2, respectively.

7. Result and discussion

On the basis of our previous papers (refs. [10, 11, 30]), this paper investigates the redistribution of the radiative energy in the case of isotropic scattering, and the RTC is derived in an absorbing, emitting and isotropic scattering parallel slab. Considering both multi-reflection and multi-scattering in the derivation, the RTC accommodates various boundary conditions under specular reflection: (a) both opaque boundaries; (b) one semi-transparent and one opaque boundary; and (c) both semi-transparent boundaries. The validity and high precision of the formula for the RTC are confirmed by comparison with the calculated results in refs. [17, 18, 22, 27].

This paper deduces the RTC in a one-dimensional absorbing, emitting and isotropic scattering slab with two diffuse reflecting opaque boundaries. By accumulating the RTC with the specular reflection boundary and the RTC with the diffuse reflection boundary linearly, the RTC in an absorbing, emitting and isotropic scattering medium with combined specular and diffuse reflecting boundaries is obtained.

The presented calculations and formulas for the redistribution of the scattering energy can also be applied to other radiative calculations. By use of this method, the

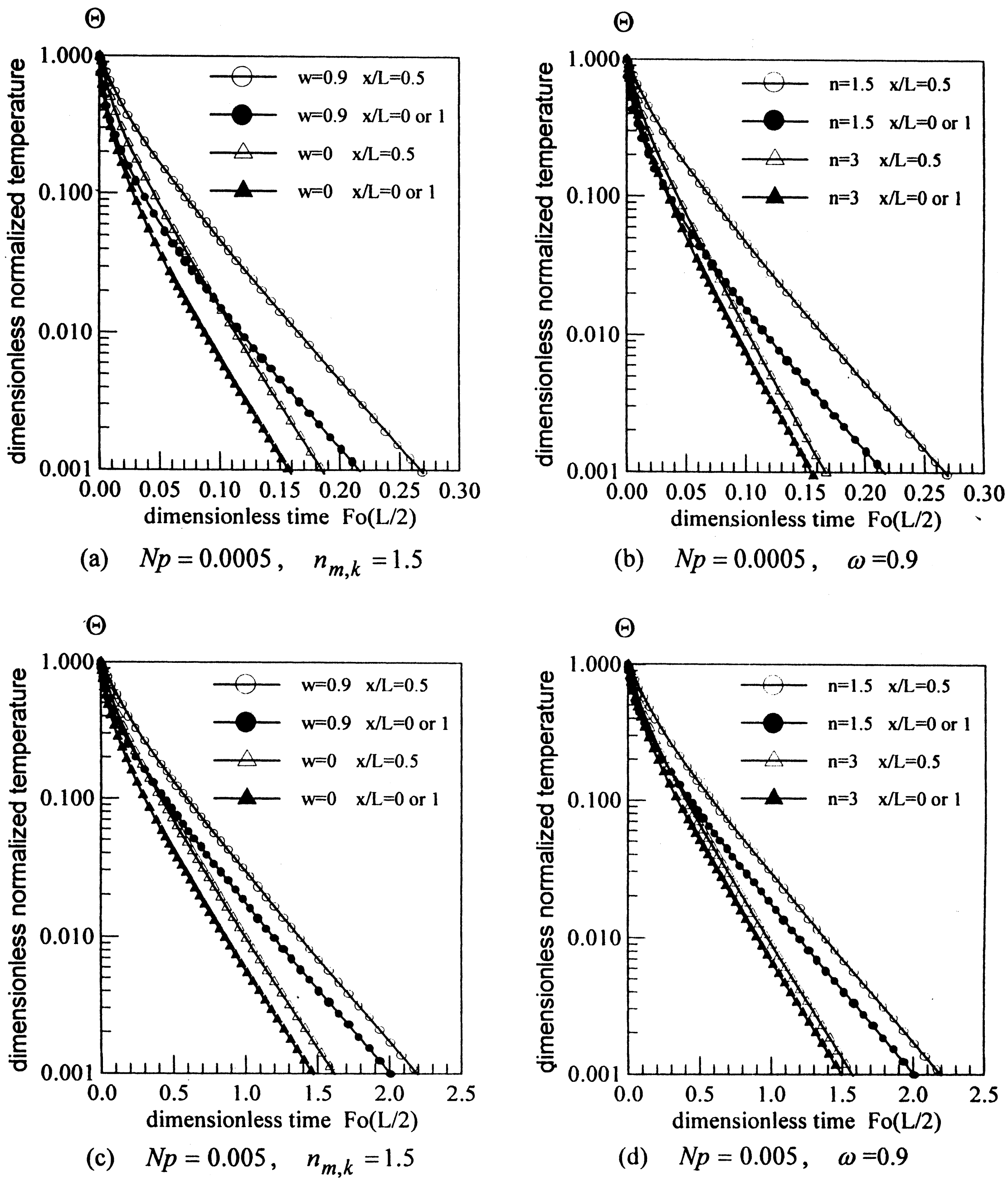

Fig. 3. Diagram of reduced temperature vs. Fourier number for various Np, refractive index and single-scattering albedo ($h_1 = h_2 = 0.08610705$, $B = 2.23\text{E}-5$, EPS0 = 3.0E−8, EPS1 = 0.0002, EPS2 = 0.001, $P_{\text{refl}} = 1$).

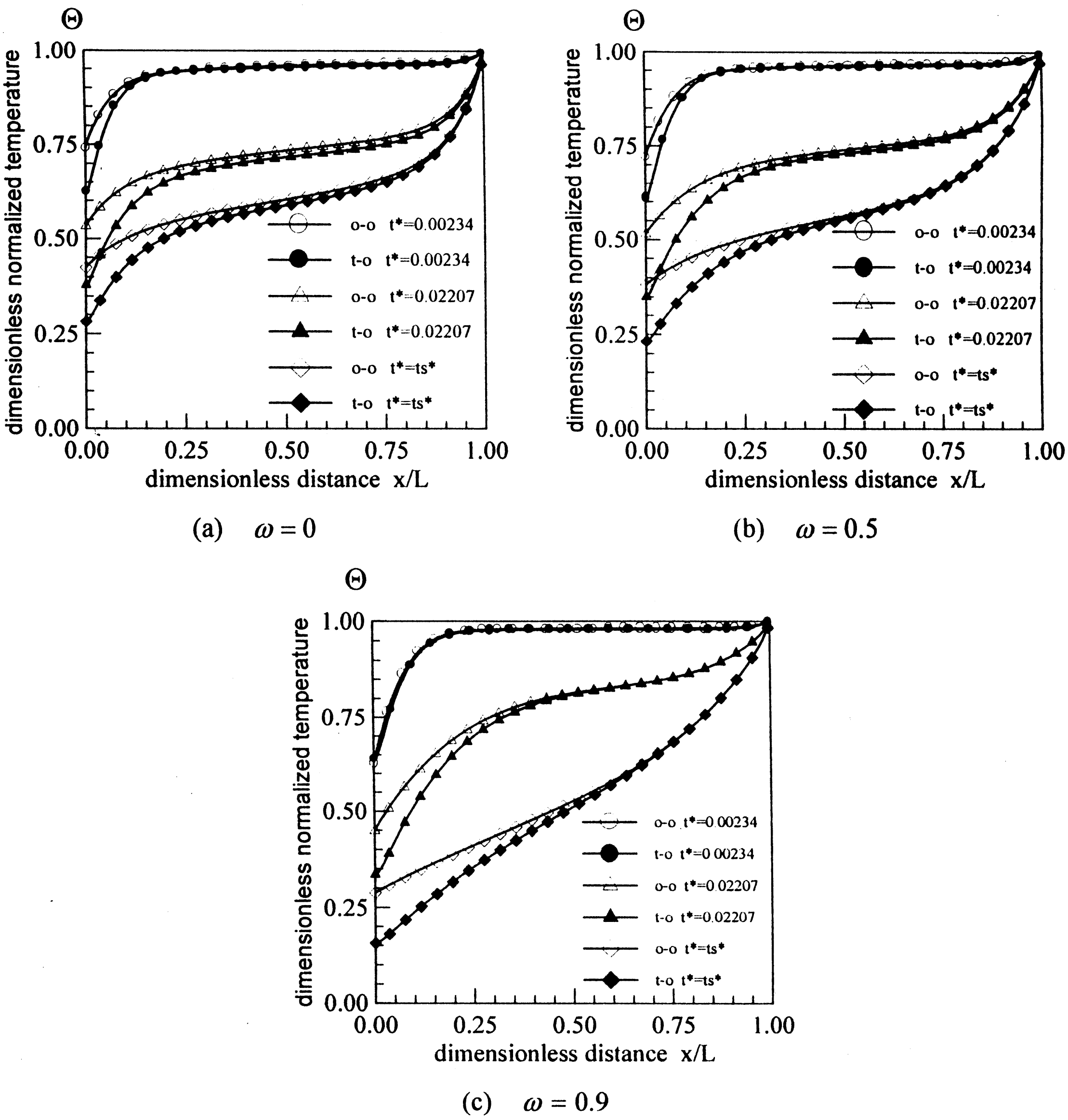

Fig. 4. Temperature profiles for mixed conditions. Comparison for opaque/opaque and semi-transparent/opaque frontiers (EPS0 = 3.0E−8, EPS1 = EPS2 = 0.0002).

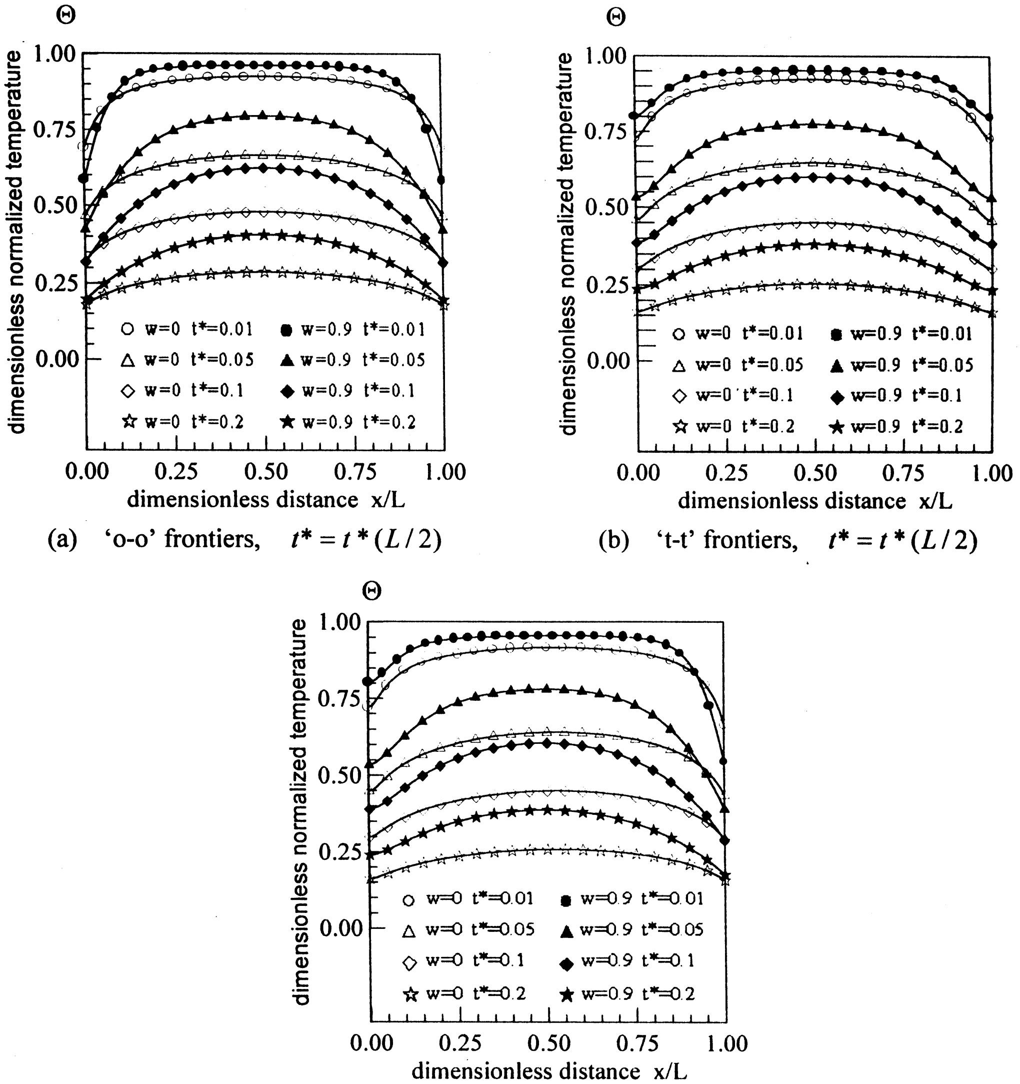

(a) 'o-o' frontiers, $t^* = t^*(L/2)$

(b) 't-t' frontiers, $t^* = t^*(L/2)$

(c) 't-o' frontiers, $t^* = t^*(L/2)$

Fig. 5. Temperature profiles for heat exchange conditions, Np ($t^* = 0$) = 0.005 and $Bi(L/2) = 0.05$. Comparison for opaque/opaque, semi-transparent/semi-transparent and semi-transparent/opaque frontiers between $\omega = 0$ and $\omega = 0.9$ ($P_{\text{refl}} = 1$, EPS0 = 3.0E−8, EPS1 = EPS2 = = 0.0005).

total radiative exchange area or total radiative transfer coefficient in a multi-dimensional non-scattering medium, which are calculated by other methods, can be developed in an isotropic scattering medium.

Acknowledgements

This research is supported by the Chinese National Science Fund for Distinguished Young Scholars (1998–2000). Our sincere gratitude goes to Professor Wang Buxuan for his useful advice.

References

[1] R. Viskanta, E.E. Anderson, Heat transfer in semi-transparent solids, in: Advances in Heat Transfer, vol. 11, Academic Press, New York, 1975, pp. 317–441.

[2] T. Kunc, M. Lallemand, J.B. Saulnier, Some new developments on coupled radiative–conductive heat transfer in glasses—experiments and modelling, Int. J. Heat Mass Transfer 27 (12) (1984) 2307–2319.

[3] R. Siegel, F.B. Molls, Finite difference solution for transient radiative cooling of a conducting semi-transparent square region, Int. J. Heat Mass Transfer 35 (10) (1992) 2579–2592.

[4] Y.L. Bao, L. Li, H.P. Tan, Q.Z. Yu, The transient three-dimensional combined radiative–conductive heat transfer in semi-transparent non-gray medium, in: B.X. Wang, (Ed.), Transport Phenomena Science and Technology, Beijing, China, 1992, pp. 553–558.

[5] S.W. Baek, T.Y. Kim, J.S. Lee, Transient cooling of a finite cylindrical medium in the rarefied cold environment, Int. J. Heat Mass Transfer 36 (16) (1993) 3949–3956.

[6] C.Y. Wu, N.R. Ou, Transient two-dimensional radiative and conductive heat transfer in a scattering medium, Int. J. Heat Mass Transfer 37 (1994) 2675–2686.

[7] W.W. Yuen, E.E. Takara, Development of a generalized zonal method for the analysis of radiative transfer in absorbing and anisotropically-scattering media, Numerical Heat Transfer, Part B 25 (1994).

[8] T.W. Tong, D.W. Yarbrough, D.L. McElroy, Y.M. Hou, Transient conductive and radiative heat transfer through a porous layer with one boundary subject to a time-varying temperature conduction, Thermal Conductivity 19 (1987) 467–479.

[9] D.E. Glass, M.N. Ozisik, D.S. McRae, Combined conduction and radiation with flux boundary condition for a semi-transparent medium covered by thin radiating layers, J. Quant. Spectrosc. Radiat. Transfer 38 (3) (1987) 201–208.

[10] H.P. Tan, Qizheng Yu, M. Lallemand, Transient combined radiative–conductive heat transfer at high temperature in semi-transparent materials, J. Eng. Thermophy. 10 (3) (1989) 295–300 (in Chinese).

[11] H.P. Tan, M. Lallemand, Transient radiative–conductive heat transfer in flat glasses submitted to temperature, flux and mixed boundary conditions, Int. J. Heat Mass Transfer 32 (5) (1989) 795–810.

[12] J.H. Tsai, J.D. Lin, Transient combined conduction and radiation with anisotropic scattering, AIAA J. Thermophysics and Heat Transfer 4 (1) (1990) 92–97.

[13] R. Siegel, Transient heat transfer in a semi-transparent radiating layer with boundary convection and surface reflections, Int. J. Heat Mass Transfer 39 (1) (1996) 69–79.

[14] O. Hahn, F. Raether, M.C. Arduini-Schuster, J. Fricke, Transient coupled conductive/radiative heat transfer in absorbing, emitting and scattering media: application to laser-flash measurement on ceramic materials, Int. J. Heat Mass Transfer 40 (3) (1997) 689–698.

[15] C.M. Spuckler, R. Siegel, Refractive index and scattering effects on radiative behavior of a semi-transparent layer, AIAA J. Thermophysics and Heat Transfer 7 (2) (1993) 302–310.

[16] C.M. Spuckler, R. Siegel, Refractive index and scattering effects on radiation in a semi-transparent laminated layer, AIAA J. Thermophysics and Heat Transfer 8 (2) (1994) 193–201.

[17] R. Siegel, Transient radiative cooling of a droplet-filled layer, ASME J. Heat Transfer 109 (2) (1987) 159–164.

[18] R. Siegel, Separation of variables solution for non-linear radiative cooling, Int. J. Heat Mass Transfer 30 (5) (1987) 959–965.

[19] J.R. Tsai, M.N. Ozisik, F. Santarelli, Radiation in spherical symmetry with anisotropic scattering and variable properties, J. Quant. Spectrosc. Radiat. Transfer 42 (3) (1989) 187–199.

[20] K. Kudo, H. Taniguchi, T. Fukuchi, Radiative heat transfer analysis in emitting–absorbing–scattering media by the Monte Carlo method (anisotropic scattering effects), Heat Transfer Japanese Research 18 (4) (1989) 87–97.

[21] H.F. Machali, Radiative transfer in participating media under conditions of radiative equilibrium, J. Quant. Spectrosc. Radiat. Transfer 53 (2) (1995) 201–210.

[22] H.F. Machali, M.A. Madkour, Radiative transfer in a participating slab with anisotropic scattering and general boundary conditions, J. Quant. Spectrosc. Radiat. Transfer 54 (5) (1995) 803–813.

[23] B.D. Ganapol, Radiative transfer in a semi-infinite medium with a specularly reflecting boundary, J. Quant. Spectrosc. Radiat. Transfer 53 (3) (1995) 257–267.

[24] Jenn-Der Lin, Jen-Hui Tsai, Radiation–conduction interaction in a planar, anisotropically scattering medium with flux boundary, Numerical Heat Transfer, Part A 16 (1989) 119–128.

[25] Qiangsheng Yang, Jie Wang, The solution of coupled conductive–radiative heat transfer with linear scattering, J. Eng. Thermophy. 11 (4) (1990) 434–437 (in Chinese).

[26] C.E. Siewert, An improved iterative method for solving a class of coupled conductive–radiative heat transfer problems, J. Quant. Spectrosc. Radiat. Transfer 54 (4) (1995) 599–605.

[27] J.I. Frankel, Cumulative variable formulation for transient conductive and radiative transport in participating medium, AIAA J. Thermophysics and Heat Transfer 9 (2) (1995) 210–218.

[28] V.A. Petrov, Combined radiation and conduction heat transfer in high temperature fiber thermal insulation, Int. J. Heat Mass Transfer 40 (1997) 2241–2247.

[29] R. Siegel, Transient thermal effects of radiant energy in translucent materials, ASME J. Heat Transfer 120 (1) (1998) 4–23.

[30] H.P. Tan, M. Lallemand, Transient combined conductive radiative heat transfer in semi-transparent materials with flux and mixed boundary conditions for semi-transparent or opaque frontiers, Eurotherm Seminar No. 1, Mons, Belgium, 1988, 7–8 March.